Clinical and Experimental Immunology ORIGINAL ARTICLE doi:10.1111/j.1365-2249.2006.03056.x

Cerebral leucocyte infiltration in lupus-prone MRL/MpJ-fas^{lpr} mice – roles of intercellular adhesion molecule-1 and P-selectin

W. G. James,* P. Hutchinson,* D. C. Bullard† and M. J. Hickey*
*Centre for Inflammatory Diseases, Monash University, Victoria, Australia, and †Department of Genetics, University of Alabama at Birmingham, Birmingham, AL, USA

Accepted for publication 25 January 2006
Correspondence: Michael J. Hickey PhD, Centre for Inflammatory Diseases, Monash University Department of Medicine, Monash Medical Centre, 246 Clayton Road, Clayton, Vic., 3168 Australia.
E-mail: michael.hickey@med.monash.edu.au

Summary

The autoimmune disease which affects MRL/MpJ-*fas*^{lpr} mice results in cerebral leucocyte recruitment and cognitive dysfunction. We have previously observed increased leucocyte trafficking in the cerebral microcirculation of these mice; however, the types of leucocytes recruited have not been analysed thoroughly, and the roles of key endothelial adhesion molecules in recruitment of these leucocytes have not been investigated. Therefore the aim of this study was to classify the phenotypes of leucocytes present in inflamed brains of MRL/MpJ-*fas*^{lpr} mice, and dissect the roles of endothelial adhesion molecules in their accumulation in the brain. Immunohistochemical analysis revealed significant leucocyte infiltration in the brains of 16- and 20-week-old MRL/MpJ-*fas*^{lpr} mice, affecting predominantly the choroid plexus. Isolation of brain-infiltrating leucocytes revealed that lymphocytes and neutrophils were the main populations present. The CD3$^+$ lymphocytes in the brain consisted of similar proportions of CD4$^+$, CD8$^+$ and CD4$^-$/CD8$^-$ [double negative (DN)] populations. Assessment of MRL/MpJ-*fas*^{lpr} mice deficient in endothelial adhesion molecules intercellular adhesion molecule-1 (ICAM-1) or P-selectin indicated that cerebral leucocyte recruitment persisted in the absence of these molecules, with only minor changes in the phenotypes of infiltrating cells. Together these data indicate that the brains of MRL/MpJ-*fas*^{lpr} mice are affected by a mixed leucocyte infiltrate, of which the unusual DN lymphocyte phenotype contributes a substantial proportion. In addition, endothelial adhesion molecules ICAM-1 and P-selectin, which modulate survival of MRL/MpJ-*fas*^{lpr} mice, do not markedly inhibit leucocyte entry into the central nervous system.

Keywords: brain, leucocyte recruitment, systemic lupus erythematosus

Introduction

Systemic lupus erythematosus (SLE) is a debilitating autoimmune disease in which a range of organs are targeted by a damaging inflammatory response. One of the organs affected most commonly in SLE patients is the central nervous system (CNS) [1]. Indeed, SLE patients can exhibit symptoms ranging from mild cognitive dysfunction to seizures and strokes [2,3]. There is a growing body of evidence that the local inflammatory response contributes to the development of these symptoms. Pathological assessment of brains from SLE patients show evidence of inflammation, with widespread microinfarcts and perivascular lymphocytic cuffing being common post mortem findings [1,4,5]. However, the mechanisms of the cerebral inflammatory response in SLE patients are poorly understood.

Much information about the inflammatory mechanisms of systemic autoimmune disease has come from the analysis of a number of spontaneous murine models, in particular the MRL/MpJ-*fas*^{lpr} mouse. Indeed, this mouse strain is used routinely as a model of SLE. MRL/MpJ-*fas*^{lpr} mice develop a severe autoimmune disease with many similarities to that seen in SLE patients, including autoantibody production, immune complex formation and systemic inflammation [6]. Furthermore, multiple lines of evidence indicate that the CNS in these animals is also affected by this disease. Behavioural studies in MRL/MpJ-*fas*^{lpr} mice have demonstrated cognitive impairments which increase in severity as the disease progresses [7–9]. In addition, the brains of these animals display extensive leucocyte infiltration and evidence of leakage of plasma proteins into the parenchyma of the brain [10]. In order to examine the mechanisms responsible for

the accumulation of leucocytes in the brains of lupus-prone mice, we recently used intravital microscopy to examine the intact cerebral (pial) microvasculature of MRL/MpJ-*fas*^{lpr} mice [11]. Post-capillary venules in the cerebral microvasculature of these mice readily supported rolling and adhesive interactions with blood-borne leucocytes during the active phase of disease, in marked contrast to the rarity of these interactions in similarly aged, non-diseased MRL$^{+/+}$ mice [11]. These findings indicate that the cerebral microvasculature is activated as part of the disease process in these mice. However, this study did not examine the types of leucocytes which enter the brain, and the molecular requirements for leucocyte accumulation in the CNS. Furthermore, the biology of the circulating leucocytes in MRL/MpJ-*fas*^{lpr} mice is highly unusual with many CD3$^+$ T cells lacking expression of both CD4 and CD8 [termed double negative (DN) T cells] [12]. The contribution of these leucocytes to the cerebral leucocyte infiltrate is unclear.

Examination of MRL/MpJ-*fas*^{lpr} mice lacking key adhesion molecules has provided strong evidence for the important roles of adhesion molecules in disease-associated pathology. Deletion of intercellular adhesion molecule-1 (ICAM-1) has been shown to increase survival and reduce leucocyte infiltration into inflamed organs such as the kidney [13,14]. In addition, absence of the ICAM-1 ligand, lymphocyte function-associated antigen-1 (LFA-1/CD11a), resulted in comparable improvements in survival and reductions in disease severity [15]. Together these findings demonstrate that interactions mediated by ICAM-1/LFA-1 play central roles in the development of inflammatory disease in MRL/MpJ-*fas*^{lpr} mice. However, it is noteworthy that this does not extend to all adhesion molecule pathways. MRL/MpJ-*fas*^{lpr} mice lacking P-selectin are not protected from early lethality and leucocyte recruitment to organs such as the kidney proceeds unabated in these animals [16,17]. Despite these studies, the roles of these adhesion molecules in promoting leucocyte entry into the brain have not been investigated. Therefore, the aims of this study were to characterize fully the phenotype of the leucocytes which enter the brains of lupus-prone MRL/MpJ-*fas*^{lpr} mice, and examine the contribution of ICAM-1 and P-selectin to the accumulation of leucocytes in the CNS.

Materials and methods

Animals

MRL/MpJ-*fas*^{lpr} mice and MRL/MpJ (MRL$^{+/+}$) were purchased from the Jackson Laboratory (Bar Harbor, ME, USA). ICAM-1$^{-/-}$ MRL/MpJ-*fas*^{lpr} mice were generated by backcrossing a gene-targeted mutation on to the MRL/MpJ-*fas*^{lpr} strain background, as described previously [13]. A similar approach was used to generate the P-selectin$^{-/-}$ MRL/MpJ-*fas*^{lpr} mice [16,17]. Mice were used at 8, 16 and 20–25 weeks of age and weighed 30–50 g.

Antibodies

The antibodies used for flow cytometry were purchased from BD Biosciences (San Diego, CA, USA) and directed against murine antigens: 30-F11 – anti-CD45, conjugated to allophycocyanin (APC); 17A2 – anti-CD3, conjugated to fluorescein isothiocyanate (FITC) or phycoerythrin (PE); GK1·5 – anti-CD4, conjugated to PE; 53–6·7 – anti-CD8a, conjugated to APC; RB6–8C5 – anti-Ly-6G (Gr-1), conjugated to PE; RA3–6B2 – anti-B220, conjugated to FITC; KT3 – anti-CD3 and M1/70 – anti-Mac-1, both purified from hybridoma supernatant and conjugated to Alexa 488 (Molecular Probes, Eugene, OR, USA).

Immunohistochemical analysis of brain leucocyte infiltration

The location of leucocytes present in the brains of lupus-prone mice was determined by immunohistochemical staining for the pan-leucocyte marker CD45. Briefly, anaesthetized mice were killed via intracardiac perfusion with phosphate-buffered saline (PBS), then fixed by perfusion with cold paraformaldehyde/lysine/periodate (PLP) fixative. Brains were removed and cryoprotected in 20% sucrose and embedded in optimum cutting temperature (OCT) embedding compound. Brains were frozen in a bath of isopentane suspended over liquid nitrogen (LN_2) then submerged in LN_2. Coronal cryostat sections (10 μm) were cut from the anterior end of the brain and 10 sections were collected at 200 μm intervals, taking the first section at the most anterior position of the ventricles. CD45$^+$ leucocytes in brain sections were identified using a modified three-layer immunohistochemistry technique [18]. Briefly, sections were blocked with normal swine serum then incubated with anti-CD45 (clone 30F-11, BD Biosciences, 1 μg/ml, overnight, 4°C). Sections were then treated with secondary antibody (rabbit anti-rat IgG), tertiary antibody [horseradish peroxidase (HRP)-conjugated sheep anti-rabbit IgG] and developed with diaminobenzidine and counterstained with haematoxylin, as described previously [18].

Analysis of anti-CD45-stained brain sections

In accord with previous data, leucocyte infiltration was located predominantly in the choroid plexus [10]. Therefore, two aspects of this region were examined in detail: (i) the area of the choroid plexus and (ii) the number of CD45$^+$ leucocytes present within the choroid plexus. The area of the choroid plexus was measured in five sections of the brain between 1000 and 2000 μm from the anterior aspect of the ventricles. Sections were examined on a Leica BMLB laboratory microscope. Images were captured at 50× magnification using a Leica DC 300F digital camera and Photoshop CS software (Adobe Systems, San Jose, CA, USA). The area of the choroid plexus was measured using Scion Image

image analysis software, following calibration using a stage micrometer, and expressed as mean area of each choroid plexus villus. The number of $CD45^+$ leucocytes in each villus (examined at 400× magnification) was also counted, and expressed relative to the villus area (cells/mm^2). The CNS parenchyma was also assessed for leucocyte infiltration in multiple high-power fields.

Isolation and identification of leucocytes in the CNS

Leucocytes present in the brain and spinal cords of $MRL^{+/+}$, MRL/MpJ-*fas*^{lpr}, P-selectin$^{-/-}$ MRL/MpJ-*fas*^{lpr} and ICAM-$1^{-/-}$ MRL/MpJ-*fas*^{lpr} mice were isolated and analysed by flow cytometry using a modification of a previously described technique [19,20]. Briefly, anaesthetized mice were killed by intracardiac perfusion of 15 ml cold PBS. The brain and spinal cord were then removed, and dissociated by passing through wire mesh. The resultant cell suspension was separated on a 90%/37%/30% Percoll (Amersham Biosciences AB, Uppsala, Sweden) gradient, and the leucocyte fraction isolated from the 90%/37% interface. Leucocytes were washed in PBS/1·0% bovine serum albumin (BSA) three times. Aliquots (100 μl) of the resultant cell suspension were incubated in one of the three following antibody combinations: (1) CD45-APC, Gr-1-PE, M1/70-FITC; (2) CD45-APC, CD3-PE, B220-FITC; (3) CD3-FITC, CD4-PE and CD8-APC. Cells were incubated for 20 min at room temperature, washed and then fixed in 4% neutral buffered formalin. Labelled cells were analysed using a MoFlo flow cytometer (Cytomation, Fort Collins, CO, USA).

To identify leucocytes from within the cell fraction isolated from the brain, cells were gated on positive staining for the leucocyte common antigen, CD45. $CD45^+$ subpopulations were classified subsequently as follows: granulocytes, Gr-1^{hi}/M1/70^{hi}; monocytes, Gr-1^{int}/M1/70^{hi}; T cells, $CD3^+$; B cells $B220^+/CD3^-$, in accord with previous observations in mice [21]. The number of cells of each subpopulation was expressed as a percentage of $CD45^+$ cells in the sample. $CD3^+$ T cells were defined further as $CD4^+$, $CD8^+$ or $CD4^-/CD8^-$ (DN), a leucocyte population observed routinely in MRL/MpJ-*fas*^{lpr} mice [12], and expressed as a percentage of $CD3^+$ cells.

Flow cytometric analysis of circulating leucocytes

To identify the leucocyte populations present in the blood of lupus-prone mice, 100 μl samples of whole blood were incubated with the same combinations of antibodies used for the brain samples. Samples underwent subsequent erythrocyte lysis and fixation using a Q-prep Workstation (Beckman Coulter, Miami, FL, USA) and flow cytometric analysis using identical conditions to the brain samples. The numbers of each cell type present in the blood were determined by reference to the circulating leucocyte counts of each animal.

Statistics

Comparisons between mouse strains were performed using Student's *t*-tests, using Bonferroni's calculation to correct for multiple comparisons. $P < 0{\cdot}05$ was deemed significant.

Results

Comparison of the phenotypes of circulating leucocytes in $MRL^{+/+}$ and MRL/MpJ-*fas*^{lpr} mice revealed that at 8 weeks, the numbers of neutrophils, monocytes, CD4 and CD8 T cells and B cells were significantly lower in MRL/MpJ-*fas*^{lpr} mice (Tables 1 and 2). In $MRL^{+/+}$ mice, leucocyte counts remained relatively stable to 20 weeks. In contrast, in MRL/MpJ-*fas*^{lpr} mice at 16 weeks, there was a marked increase in the number of circulating leucocytes. Much of this change was due to a striking elevation in circulating T cells of almost 10×10^6/ml, with an increase in circulating DN T cells accounting for the majority of this difference. In $MRL^{+/+}$ mice, DN T cells represented a very minor population. Small but significant increases in neutrophils and monocytes were also observed in 16-week MRL/MpJ-*fas*^{lpr} mice (Tables 1 and 2). By 20 weeks, the leucocyte counts in MRL/MpJ-*fas*^{lpr} mice had undergone a further increase to nearly 30×10^6/ml, with more than 14×10^6/ml being DN T cells.

Leucocyte infiltration is elevated in the choroid plexus of MRL/MpJ-fas^{lpr} mice

Histological examination of leucocyte infiltration in brains of MRL/MpJ-*fas*^{lpr} mice revealed that, in accord with previous observations, the choroid plexus was the primary site of leucocyte infiltration (Fig. 1), with leucocytes rarely detectable within the parenchyma [10]. Therefore, detailed comparison of $MRL^{+/+}$ and MRL/MpJ-*fas*^{lpr} mice was based on analysis of the choroid plexus. In $MRL^{+/+}$ mice, the villi of the choroid plexus were thin and contained diffuse areas of $CD45^+$ cell infiltration (Fig. 1a). In contrast, the intensity of infiltration in the choroid plexus of MRL/MpJ-*fas*^{lpr} mice was such that the size of the villi appeared increased relative to $MRL^{+/+}$ mice (Fig. 1b). We therefore quantified the size of the choroid plexus villi and intensity of infiltration of the choroid in $MRL^{+/+}$ and MRL/MpJ-*fas*^{lpr} mice. At 16 weeks, the mean area of the choroid plexus in MRL/MpJ-*fas*^{lpr} mice was greater than twice that in $MRL^{+/+}$ mice ($P < 0{\cdot}05$) (Fig. 2a). Moreover, by 20 weeks, both the area of the choroid villi and the number of leucocytes per mm^2 of choroid villus area were significantly greater in MRL/MpJ-*fas*^{lpr} mice relative to $MRL^{+/+}$ mice (Fig. 2c,d).

Neutrophils and T cells are the dominant leucocytes recruited to the brains of MRL/MpJ-fas^{lpr} mice

The infiltrating leucocytes in brains of MRL/MpJ-*fas*^{lpr} mice were then purified from the brain via density gradient

Table 1. Circulating leucocyte counts and leucocyte subsets in MRL$^{+/+}$, MRL/MpJ-*fas*^{lpr}, P-selectin$^{-/-}$ -MRL/MpJ-*fas*^{lpr}, and intercellular adhesion molecule-1 (ICAM-1)$^{-/-}$ -MRL/MpJ-*fas*^{lpr} mice at 8, 16 and 20–25 weeks of age.*

	Total	M1/70^{hi}/Gr-1^{hi} (PMNs)	M1/70^{hi}/Gr-1^{int} (monocyte lineage)	CD3$^+$ (T cells)	B220$^+$/CD3$^-$ (B cells)
MRL$^{+/+}$					
8 weeks	6·8 ± 0·5 (6)	1·5 ± 0·1 (6)	0·20 ± 0·28 (6)	3·2 ± 0·3 (6)	2·1 ± 0·2 (6)
16 weeks	7·4 ± 0·5 (6)	1·6 ± 0·1 (6)	0·20 ± 0·01 (6)	3·2 ± 0·2 (6)	1·7 ± 0·1 (6)
20–25 weeks	4·9 ± 0·6 (7)	1·3 ± 0·2 (7)	0·14 ± 0·05 (7)	1·9 ± 0·2 (7)	0·9 ± 0·2 (7)
MRL/MpJ-fas^{lpr}					
8 weeks	5·3 ± 0·4 (6)	0·9 ± 0·1 (6)†	0·07 ± 0·01 (6)†	2·0 ± 0·1 (9)†	1·0 ± 0·1 (9)†
16 weeks	19·4 ± 3·8 (6)	4·5 ± 0·9 (6)†	0·77 ± 0·17 (6)†	12·8 ± 1·3 (6)†	1·4 ± 0·1 (6)
20–25 weeks	29·6 ± 4·1 (7)	5·3 ± 1·8 (6)†	0·72 ± 0·18 (6)†	20·8 ± 1·6 (6)†	2·0 ± 0·2 (6)†
P-selectin$^{-/-}$-MRL/MpJ-fas^{lpr}					
8 weeks	10·9 ± 0·5 (9)	4·4 ± 0·3 (8)**	0·56 ± 0·07 (8)**	3·1 ± 0·4 (6)**	1·7 ± 0·3 (6)**
16 weeks	20·2 ± 4·9 (5)	5·7 ± 0·7 (6)	0·79 ± 0·14 (6)	10·7 ± 0·8 (8)	2·8 ± 0·2 (8)**
20–25 weeks	27·8 ± 4·9 (6)	6·5 ± 1·6 (6)	0·72 ± 0·16 (6)	14·6 ± 1·6 (7)**	3·1 ± 0·4 (7)**
ICAM-1$^{-/-}$-MRL/MpJ-fas^{lpr}					
16 weeks	16·1 ± 4·4 (5)	3·2 ± 0·8 (6)	0·50 ± 0·13 (6)	7·3 ± 0·7 (8)**	2·0 ± 0·2 (8)**
20–25 weeks	28·7 ± 6·7 (5)	4·3 ± 0·8 (6)	0·51 ± 0·09 (6)	18·1 ± 0·8 (6)	4·7 ± 0·7 (6)**

*Data are expressed as cells × 10^6/ml ± s.e.m. The number of mice sampled is shown in parentheses. †$P < 0·05$ *versus* MRL$^{+/+}$ at same age. **$P < 0·05$ *versus* MRL/MpJ-*fas*^{lpr} at same age.

centrifugation and identified using flow cytometry. At both 16 and 20 weeks, the dominant cell types present in the brains were neutrophils and lymphocytes, together comprising 70–80% of the CD45$^+$ leucocyte population (Fig. 3). Monocytes and B cells each comprised < 10% of the infiltrated leucocytes. It must be noted that, in many cases, the total leucocyte percentages did not reach 100%. Given that this was not observed when leucocytes were isolated from blood, this suggests that the process of brain dissociation and leucocyte isolation induced loss of one of the surface markers used for leucocyte identification. We next examined the T lymphocyte populations present in the brain (Fig. 4). At 16 weeks, the numbers of CD4$^+$, CD8$^+$ and DN cells were similar (Fig. 4a). At 20 weeks the number of CD4$^+$ cells was higher than the other two populations; however, both CD8 and DN populations were present in substantial numbers (Fig. 4b). These data indicate that DN T cells are able to exit the cerebral vasculature and enter the brain to a similar extent as the other T cell phenotypes.

Table 2. Phenotypes of circulating CD3$^+$ leucocytes in MRL$^{+/+}$, MRL/MpJ-*fas*^{lpr}, P-selectin$^{-/-}$ MRL/MpJ-*fas*^{lpr} and intercellular adhesion molecule-1 (ICAM-1)$^{-/-}$ MRL/MpJ-*fas*^{lpr} mice at 8, 16 and 20–25 weeks of age.*

	CD4$^+$	CD8$^+$	CD4$^-$/CD8$^-$ (DN)	B220$^+$
MRL$^{+/+}$				
8 weeks (6)	1·75 ± 0·05 (6)	1·30 ± 0·03 (6)	0·09 ± 0·02 (6)	0·98 ± 0·43 (6)
16 weeks (7)	1·50 ± 0·10 (7)	1·40 ± 0·10 (7)	0·22 ± 0·08 (7)	0·35 ± 0·11 (6)
20–25 weeks (7)	1·04 ± 0·04 (7)	0·82 ± 0·05 (7)	0·06 ± 0·02 (7)	0·05 ± 0·01 (7)
MRL/MpJ-fas^{lpr}				
8 weeks (9)	0·86 ± 0·04 (9)†	0·91 ± 0·03 (9)†	0·18 ± 0·01 (9)†	0·38 ± 0·03 (9)
16 weeks (6)	1·75 ± 0·17 (6)	2·50 ± 0·39 (6)†	8·46 ± 0·55 (6)†	9·20 ± 1·32 (6)†
20–25 weeks (6)	2·71 ± 0·18 (6)†c	3·56 ± 0·24 (6)†	14·42 ± 0·34 (6)†	14·33 ± 0·67 (6)†
P-selectin$^{-/-}$-MRL/MpJ-fas^{lpr}				
8 weeks (8)	1·44 ± 0·03 (8)**	1·44 ± 0·03 (8)**	0·24 ± 0·02 (8)**	0·54 ± 0·09 (6)**
16 weeks (6)	1·69 ± 0·23 (6)	1·52 ± 0·29 (6)**	7·43 ± 0·41 (6)	7·50 ± 0·93 (8)
20–25 weeks (7)	2·35 ± 0·18 (7)	2·06 ± 0·44 (7)**	10·17 ± 0·43 (7)**	10·76 ± 1·36 (7)**
ICAM-1$^{-/-}$-MRL/MpJ-fas^{lpr}				
16 weeks (6)	1·43 ± 0·11 (6)	1·50 ± 0·19 (6)**	4·29 ± 0·30 (6)**	3·30 ± 0·77 (8)**
20–25 weeks (6)	4·14 ± 0·23 (6)**	3·41 ± 0·12 (6)	10·49 ± 0·30 (6)**	11·73 ± 0·77 (6)**

*CD4$^+$, CD8$^+$, CD4$^-$/CD8$^-$ and B220$^+$data are expressed as cells × 10^6/ml ± s.e.m. based on the total CD3$^+$ cell count, and percentage data for each subclass. The number of mice sampled is shown in parentheses. †$P < 0·05$ *versus* MRL$^{+/+}$ at same age. **$P < 0·05$ *versus* MRL/MpJ-*fas*^{lpr} at same age.

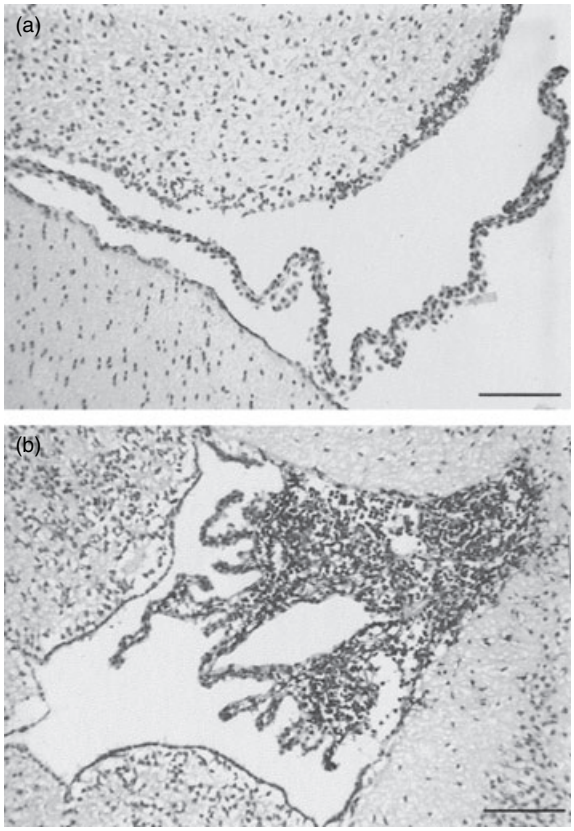

Fig. 1. Cerebral leucocyte recruitment in the brains of MRL$^{+/+}$ (a) and MRL/MpJ-*fas*^{lpr} (b) mice at 20 weeks. Intense leucocyte infiltrate is present in choroid plexus villi of MRL/MpJ-*fas*^{lpr} mice but not in MRL$^{+/+}$ mice. Bar denotes 100 μm.

Effect of ICAM-1 and P-selectin deficiency on infiltration

We next examined leucocyte infiltration in MRL/MpJ-*fas*^{lpr} mice deficient in either ICAM-1 or P-selectin. In 20-week-old mice, neither adhesion molecule deficiency resulted in a reduction in choroid leucocyte infiltration (Fig. 5). In contrast, ICAM-1$^{-/-}$ MRL/MpJ-*fas*^{lpr} mice displayed increased leucocyte recruitment, apparent as a significant increase in the density of leucocyte infiltrate within the affected area (Fig. 5b). P-selectin$^{-/-}$ mice did not differ from wild-type mice.

Assessment of the types of leucocytes present in the brains of these mice showed that at 16 weeks, a greater proportion of both T and B cells were present in brains of both ICAM-1$^{-/-}$ and P-selectin$^{-/-}$ MRL/MpJ-*fas*^{lpr} mice, relative to wild-type MRL/MpJ-*fas*^{lpr} mice (Fig. 6a). However, by 20 weeks, no differences were observed in the broad phenotypes of leucocytes in the brains of these mice (Fig. 6b). In addition, investigation of the types of T cells present revealed only minor differences in the T cell populations present (Fig. 7). At 16 weeks, ICAM-1$^{-/-}$ mice had a significantly increased proportion of CD4^{+} cells, whereas at 20 weeks, DN T cells were significantly increased in P-selectin$^{-/-}$ MRL/MpJ-*fas*^{lpr} mice, relative to wild-type MRL/MpJ-*fas*^{lpr} mice.

Effect of deficiency of ICAM-1 or P-selectin on phenotype of circulating leucocytes in MRL/MpJ-fas^{lpr} mice

Mice deficient in ICAM-1 and P-selectin on conventional backgrounds have been described previously to have increased circulating leucocyte counts [22,23]. Therefore, we examined circulating leucocyte phenotypes of these mice on the MRL/MpJ-*fas*^{lpr} background (Tables 1 and 2). At 8 weeks, P-selectin$^{-/-}$ MRL/MpJ-*fas*^{lpr} mice displayed significant elevations in all cell types, but most prominently in neutrophils. At 16 and 20 weeks, the number of circulating leucocytes in both strains showed comparable elevations (relative to MRL$^{+/+}$ mice) to those seen in wild-type MRL/MpJ-*fas*^{lpr} mice. However, ICAM-1$^{-/-}$ mice showed evidence of a delay in the increase in CD3^{+} cells, as at 16 weeks the number of CD3^{+} cells was lower than that seen in wild-type MRL/MpJ-*fas*^{lpr} mice, due to reduced numbers of CD8 and DN T cells. However, by 20 weeks, ICAM-1$^{-/-}$ mice had become similar to wild-type MRL/MpJ-*fas*^{lpr} mice, apart from an alteration in the proportions of T cells such that CD4 cells were increased significantly and DN T cells were decreased significantly (Tables 1 and 2). In P-selectin$^{-/-}$ mice at 20 weeks, the number of CD3^{+} T cells was reduced relative to the extremely high levels in wild-type MRL/MpJ-*fas*^{lpr} mice, due to lower levels of CD8 and DN T cells in P-selectin$^{-/-}$ mice (Tables 1 and 2). Finally, DN T cells in MRL/MpJ-*fas*^{lpr} mice have been observed previously to express B220 [24]. Examination of

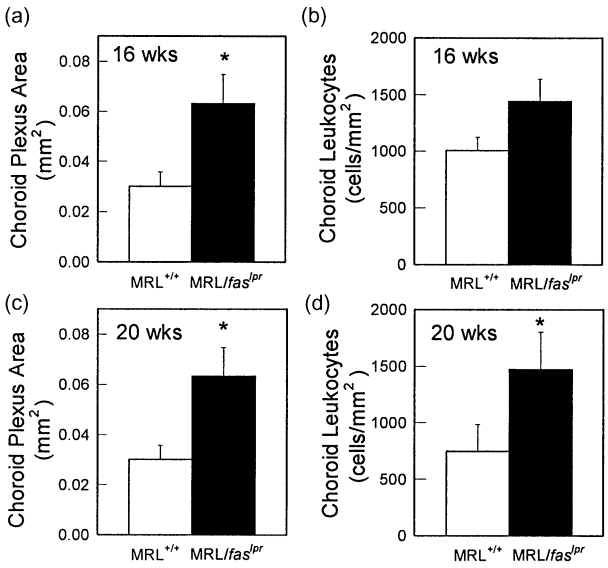

Fig. 2. Quantification of leucocyte recruitment in the choroid plexus of MRL$^{+/+}$ and MRL/MpJ-*fas*^{lpr} mice at 16 and 20 weeks. Brains were sectioned at regular intervals and leucocyte recruitment identified using immunohistochemistry for CD45. (a,c) Area of the choroid plexus in MRL$^{+/+}$ and MRL/MpJ-*fas*^{lpr} mice at 16 (a)and 20 (c)weeks. (b,d) Density of CD45^{+} leucocyte infiltrate present in the choroid plexus of both mouse strains at 16 (b) and 20 (d)weeks. $n = 6$–8 mice per group. Data are shown as mean ± s.e.m. *$P < 0{\cdot}05$ *versus* MRL$^{+/+}$ mice.

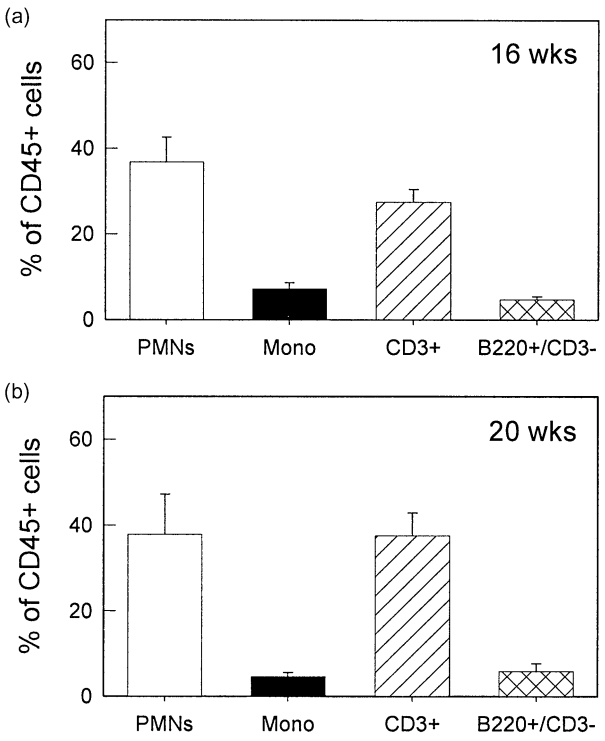

Fig. 3. Leucocyte phenotypes present in brains of MRL/MpJ-*fas*^{lpr} mice at 16 and 20 weeks. Leucocytes were isolated from brains using density centrifugation and classified using flow cytometry as follows: PMNs – Gr-1^{hi}/M1/70^{hi}; monocytes – Gr-1^{int}/M1/70^{hi}; T cells – CD3^{+}; B cells – B220^{+}/CD3^{-}. $n = 7$–13 mice per group. Data are shown as mean ± s.e.m.

B220 expression on CD3^{+} cells in the present study revealed that the number of B220^{+} CD3^{+} lymphocytes was very similar to the number of DN T cells, suggesting that all circulating DN T cells in all strains of MRL/MpJ-*fas*^{lpr} mice examined expressed B220 (Table 2).

Discussion

It has been assumed that leucocytes rarely enter the brain, due to the nature of the blood–brain barrier. However, it is clear that in response to local inflammatory stimuli leucocytes can gain access readily to the brain [20,25–27]. This also applies in the systemic disease which affects the MRL/MpJ-*fas*^{lpr} mouse [10,28]. Moreover, the finding that immunosuppressive treatments which reduce cerebral leucocyte infiltration protect MRL/MpJ-*fas*^{lpr} mice from cognitive dysfunction provides support for the concept that leucocytes are key contributors to cerebral pathology in these lupus-prone mice [29]. However, the mechanisms responsible for this leucocyte recruitment are unknown. We have demonstrated previously that the cerebral microvasculature of MRL/MpJ-*fas*^{lpr} mice shows evidence of aberrant activation, such that leucocyte–endothelial cell interactions are increased relative to non-diseased mice [11]. Due to the extremely low rate of leucocyte trafficking in the uninflamed brain, it is probable that in diseased MRL/MpJ-*fas*^{lpr} mice this endothelial activation is critical to allowing large numbers of leucocytes to attach to the cerebral endothelium and exit the vasculature.

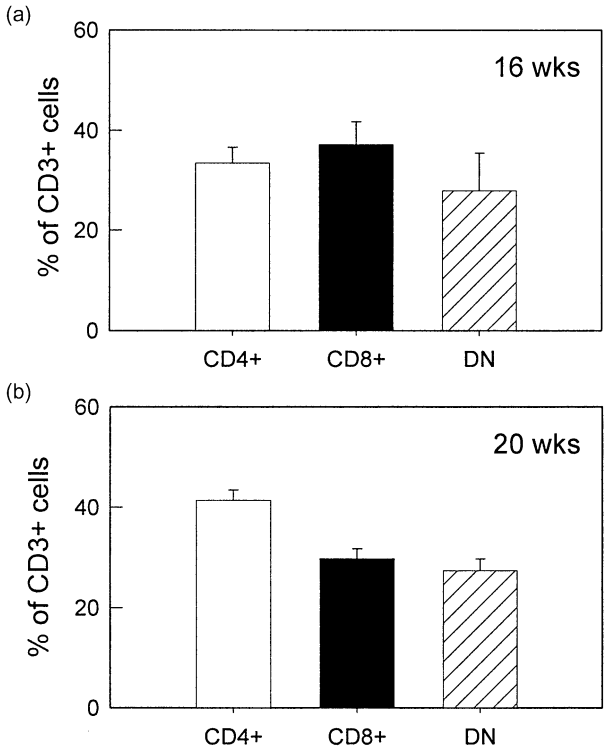

Fig. 4. T cell phenotypes present in brains of MRL/MpJ-*fas*^{lpr} mice at 16 and 20 weeks. Leucocytes were isolated from brains using density centrifugation and CD3^{+} leucocytes were classified using flow cytometry as CD4^{+}, CD8^{+} or CD4^{-}/CD8^{-} (DN). $n = 6$ mice per group. Data are shown as mean ± s.e.m.

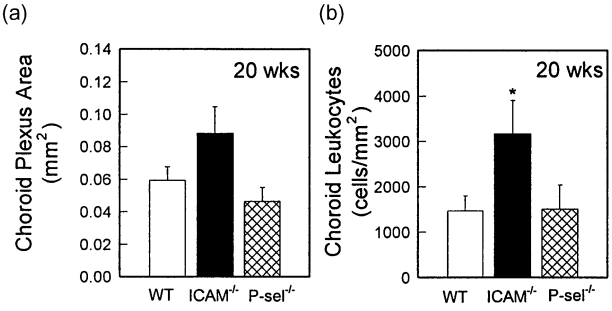

Fig. 5. Quantification of leucocyte recruitment in the choroid plexus of wild-type (WT) MRL/MpJ-*fas*^{lpr} mice and intercellular adhesion molecule-1 (ICAM-1)$^{-/-}$ and P-selectin$^{-/-}$ MRL/MpJ-*fas*^{lpr} mice at 20 weeks. Brains were sectioned at regular intervals and leucocyte recruitment identified using immunohistochemistry for CD45. (a) Area of choroid plexus. (b) Density of CD45^{+} leucocyte infiltrate present in the choroid plexus of each of the mouse strains. $n = 7$ for WT mice and 4 for ICAM-1$^{-/-}$ and P-selectin$^{-/-}$ mice. Data are shown as ± s.e.m. $^{*}P < 0{\cdot}05$ *versus* MRL/MpJ-*fas*^{lpr} mice.

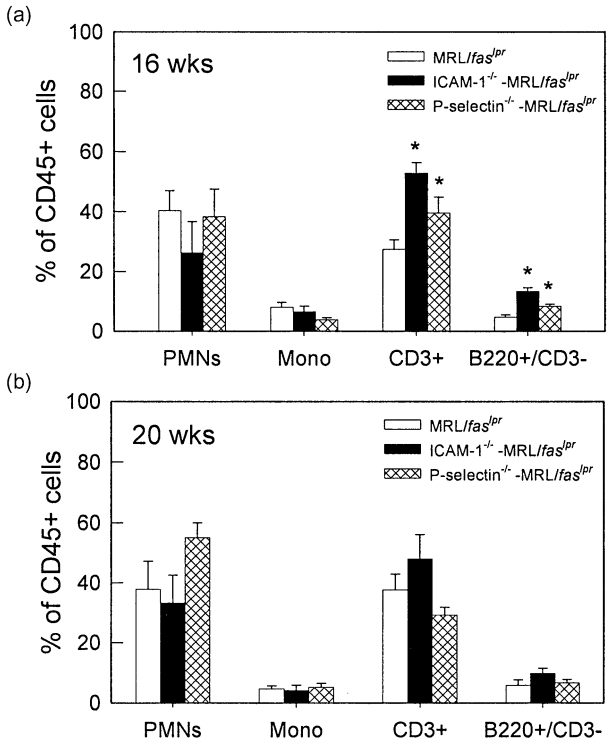

Fig. 6. Leucocyte phenotypes present in brains of wild-type, ICAM-1$^{-/-}$ and P-selectin$^{-/-}$MRL/MpJ-*fas*^{lpr} mice at 16 and 20 weeks. Leucocytes were isolated from brains using density centrifugation and classified using flow cytometry as described for Fig. 3. Data are shown as mean ± s.e.m. of 6–13 mice per group. *$P < 0{\cdot}05$ *versus* MRL/MpJ-*fas*^{lpr} mice.

Despite these studies, the endothelial adhesion molecules required for leucocyte entry into the brain remain unclear. Furthermore, the complex immunology of these mice has meant that the types of leucocytes which are recruited to these animals have not been identified clearly. Therefore, the two aims of this study were to classify the types of leucocytes recruited to the brains of these mice, and investigate the roles of two candidate adhesion molecules in their recruitment. The data show that the leucocyte infiltrate consists predominantly of a mixture of T cells and neutrophils, and that DN T cells comprise approximately one-third of all T cells. In addition, the absence of either ICAM-1 or P-selectin did not affect markedly the recruitment of the key leucocyte populations to the inflamed brains of MRL/MpJ-*fas*^{lpr} mice.

DN T cells are generated in large numbers in MRL/MpJ-*fas*^{lpr} mice [6]. Moreover, evidence indicates that they contribute significantly to tissue injury in the kidney [30]. However, DN T cells have been difficult to identify definitively using immunohistochemistry, as the main marker used to identify them (B220) is also expressed on B cells. Therefore, to investigate their contribution to cerebral leucocyte infiltration, we isolated leucocytes from the brains and used flow cytometry to examine multiple cell markers on individual cells. This allowed the unequivocal identification of CD3$^+$ DN T cells in brains of lupus mice, in addition to CD4 and CD8 single-positive cells. This demonstrated that DN T cells were able to enter the brain effectively, to the extent that they comprised approximately one-third of all T cells in the brain. Infiltration of CD4$^+$/CD8$^+$ 'double-positive' cells was also investigated, as it has been suggested that CD4$^+$ cells accumulate in the brain only because they are dysfunctional and display aberrant expression of both CD4 and CD8 [10,31]. However, in the present study double-positive cells were observed rarely in the inflamed brains of lupus mice.

The conventional paradigm used to explain the movement of leucocytes from the mainstream of blood flow into tissues requires that leucocytes first roll then adhere onto the endothelial surface, and subsequently exit the vasculature [32]. In many cases, the initial rolling interaction is selectin-mediated, whereas the subsequent adhesion step requires interaction between leucocyte integrins and their endothelial ligands, including ICAM-1 and vascular cell adhesion molecule-1 (VCAM-1) [33]. We have observed previously a key role for the α4-integrin/VCAM-1 pathway in mediating leucocyte interactions in pial post-capillary venules in MRL/MpJ-*fas*^{lpr} mice [11]. Moreover, although P-selectin mediated some rolling in cerebral microvessels, in its absence the

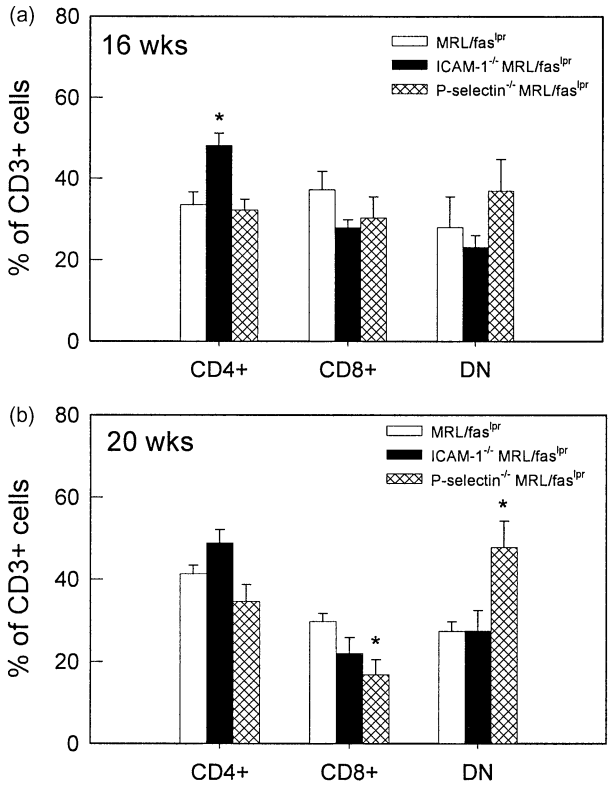

Fig. 7. T cell phenotypes present in brains of wild-type, ICAM-1$^{-/-}$ and P-selectin$^{-/-}$MRL/MpJ-*fas*^{lpr} mice at 16 and 20 weeks. Leucocytes were isolated from brains using density centrifugation and CD3$^+$ leucocytes were classified using flow cytometry as CD4$^+$, CD8$^+$ or CD4$^-$/CD8$^-$ (DN). Data are shown as mean ± s.e.m. of 5–10 mice per group. *$P < 0{\cdot}05$ *versus* MRL/MpJ-*fas*^{lpr} mice.

number of leucocytes which became adherent was unaltered. However, this study examined only intravascular rolling and adhesive interactions. The approach used did not allow assessment of the molecular basis for the subsequent step of leucocyte emigration from the vasculature. In addition, the area of the most intense cerebral leucocyte recruitment in these animals, the choroid plexus, was not examined. The molecular basis of rolling and adhesion is characterized readily, as inhibitory antibodies can block these interactions rapidly. In contrast, emigration and leucocyte accumulation in the brain is a much slower process [34]. Under these circumstances, use of MRL/MpJ-*fas*^{lpr} mice deficient in specific adhesion molecules provides an excellent tool for the assessment of the molecular basis for leucocyte accumulation in the brain. These experiments have demonstrated clearly that ICAM-1 and P-selectin are not required for leucocyte recruitment to the CNS in MRL/MpJ-*fas*^{lpr} mice.

It was noteworthy that in 20-week ICAM-1$^{-/-}$ MRL/MpJ-*fas*^{lpr} mice, leucocyte infiltration was elevated significantly relative to wild-type MRL/MpJ-*fas*^{lpr} mice, suggesting that ICAM-1 acts to reduce the numbers of leucocytes which accumulate in the CNS. The mechanisms whereby ICAM-1 may mediate this effect are not clear. Given the established role of ICAM-1 as a lymphocyte co-stimulatory molecule, the elevation in recruitment may be a consequence of altered lymphocyte activation in ICAM-1-deficient cells [35,36]. Alternatively ICAM-1 may be involved in leucocyte elimination from the inflamed brain via processes such as apoptosis or recirculation.

Deficiency in ICAM-1 has been shown previously to have a specific effect on neutrophil migration, as shown by a four-fold increase in circulating neutrophils and a concomitant decrease in neutrophil migration to sites of inflammation [22]. Similarly, deficiency in P-selectin has been reported to result in a 2·4-fold increase in circulating neutrophil numbers, and an inhibition, but not elimination, of neutrophil entry into the inflamed peritoneum [23]. The effect of deficiency of P-selectin on leucocyte recruitment is variable depending on the model investigated. In some models, the absence of P-selectin results in almost complete absence of leucocyte recruitment [37], whereas in others the absence of P-selectin does not reduce recruitment [38,39]. Studies with mice lacking both P-selectin and E-selectin have shown that additional absence of E-selectin results in a much more profound deficiency in recruitment, suggesting that in the absence of P-selectin, E-selectin can mediate critical leucocyte rolling interactions required for recruitment induced by inflammatory stimuli [40,41]. Given these findings, it is arguably not surprising that in the present experiments, leucocyte entry into the brain was not affected by either deletion. This suggests that alternative adhesion molecules may assume the roles played by P-selectin and ICAM-1 in supporting leucocyte entry into the brain. This possibility is supported by the fact that the inflammation which affects the MRL/MpJ-*fas*^{lpr} mouse occurs over several months, allowing time for expression of alternative adhesion molecule pathways.

The reason the choroid plexus is a preferential target of cerebral leucocyte recruitment in MRL/MpJ-*fas*^{lpr} mice is unclear. It is possible that the fenestrated endothelium of the choroid plexus allows leucocyte entry to occur more readily, and the preferential deposition of immune complexes in this site may also act to attract and retain leucocytes [28]. In addition, investigation of adhesion molecule expression in the choroid has demonstrated that the choroid epithelial cells, but not the associated endothelial cells, constitutively express ICAM-1 and VCAM-1, and increase expression of these molecules during inflammatory responses [42]. This finding raises the possibility that following leucocyte exit from the vasculature, epithelial cell-expressed molecules are important in retaining leucocytes at this site. It is clear from the present findings that ICAM-1 does not serve this function, as large numbers of leucocytes accumulate in the choroid plexus of ICAM-1$^{-/-}$ MRL/MpJ-*fas*^{lpr} mice. However, epithelial cell-expressed VCAM-1 could act in this fashion as many of the leucocyte types present in the choroid, including DN T cells (data not shown), express VCAM-1 ligands such as the α4-integrin, making them capable of adhering to VCAM-1-expressing cells [43,44].

Recent observations have shown that in some tissues the necessity for a rolling interaction prior to leucocyte adhesion to the endothelium is bypassed [45–47]. Furthermore, in CNS microvessels, adhesion of activated lymphoblasts has been observed to occur without prior rolling [34]. Given these findings, it is conceivable that in the choroid plexus vasculature the conventional multi-step paradigm of leucocyte recruitment does not apply. Under these circumstances it is plausible that neither P-selectin nor ICAM-1 are required for leucocyte adhesion within the choroidal vasculature. Further experiments with MRL/MpJ-*fas*^{lpr} mice lacking alternative adhesion molecules would aid in clarifying this issue.

Acknowledgements

These studies were supported by a programme grant (no. 334067) from the National Health and Medical Research Council (NHMRC), Australia and an NIH RO1 grant (no. AR51807-01), both held by M. Hickey, and an NIH grant (no. RR-017009) to D. Bullard. M. Hickey is an NHMRC R. D. Wright Fellow.

References

1 Lahita RG. Systemic lupus erythematosus, 3rd edn. San Diego: Academic Press, 1999.
2 van Dam AP. Diagnosis and pathogenesis of CNS lupus. Rheumatol Int 1991; **11**:1–11.
3 Mitsias P, Levine SR. Large cerebral vessel occlusive disease in systemic lupus erythematosus. Neurology 1994; **44**:385–93.

4 Hanly JG, Walsh NM, Sangalang V. Brain pathology in systemic lupus erythematosus. J Rheumatol 1992; **19**:732–41.
5 Osborn L, Hession C, Tizard R *et al.* Direct expression cloning of vascular cell adhesion molecule 1, a cytokine-induced endothelial protein that binds to lymphocytes. Cell 1989; **59**:1203–11.
6 Theofilopoulos AN, Dixon FJ. Murine models of systemic lupus erythematosus. Adv Immunol 1985; **37**:269–390.
7 Hess DC, Taormina M, Thompson J *et al.* Cognitive and neurologic deficits in the MRL/lpr mouse: a clinicopathologic study. J Rheumatol 1993; **20**:610–7.
8 Sakic B, Szechtman H, Talangbayan H *et al.* Disturbed emotionality in autoimmune MRL-lpr mice. Physiol Behav 1994; **56**:609–17.
9 Walker SE, Wright DC, O'Sullivan FX *et al.* Memory, learning ability, and neuropathologic status of mice with systemic lupus erythematosus. Ann NY Acad Sci 1997; **823**:107–15.
10 Vogelweid CM, Johnson GC, Besch-Williford CL *et al.* Inflammatory central nervous system disease in lupus-prone MRL/lpr mice: comparative histologic and immunohistochemical findings. J Neuroimmunol 1991; **35**:89–99.
11 James WG, Bullard DC, Hickey MJ. Critical role of the alpha 4 integrin/VCAM-1 pathway in cerebral leukocyte trafficking in lupus-prone MRL/fas(lpr) mice. J Immunol 2003; **170**:520–7.
12 Hammond DM, Nagarkatti PS, Gote LR *et al.* Double-negative T cells from MRL-lpr/lpr mice mediate cytolytic activity when triggered through adhesion molecules and constitutively express perforin gene. J Exp Med 1993; **178**:2225–30.
13 Bullard DC, King PD, Hicks MJ *et al.* Intercellular adhesion molecule-1 deficiency protects MRL/MpJ-*Fas*^{lpr} mice from early lethality. J Immunol 1997; **159**:2058–67.
14 Lloyd CM, Gonzalo J-A, Salant DA *et al.* Intercellular adhesion molecule-1 deficiency prolongs survival and protects against the development of pulmonary inflammation during murine lupus. J Clin Invest 1997; **100**:963–71.
15 Kevil CG, Hicks MJ, He X *et al.* Loss of LFA-1, but not Mac-1, protects MRL/MpJ-Fas(lpr) mice from autoimmune disease. Am J Pathol 2004; **165**:609–16.
16 He X, Panoskaltsis-Mortari A, Samuel S *et al.* P-selectin deficiency accelerates development of autoimmune disease in MRL/MpJ-Faslpr mice. FASEB J 2004; **18**:A554.
17 Hickey MJ, Bullard DC, Issekutz A *et al.* Leukocyte–endothelial cell interactions are enhanced in dermal postcapillary venules of MRL/*fas*^{lpr} (lupus-prone) mice: roles of P- and E-selectin. J Immunol 2002; **168**:4728–36.
18 Huang XR, Holdsworth SR, Tipping PG. Evidence for delayed-type hypersensitivity mechanisms in glomerular crescent formation. Kidney Int 1994; **46**:69–78.
19 Krakowski ML, Owens T. The central nervous system environment controls effector CD4$^+$ T cell cytokine profile in experimental allergic encephalomyelitis. Eur J Immunol 1997; **27**:2840–7.
20 Kerfoot SM, Kubes P. Overlapping roles of P-selectin and alpha(4) integrin to recruit leukocytes to the central nervous system in experimental autoimmune encephalomyelitis. J Immunol 2002; **169**:1000–6.
21 Lagasse E, Weissman IL. Flow cytometric identification of murine neutrophils and monocytes. J Immunol Meth 1996; **197**:139–50.
22 Sligh JE Jr, Ballantyne CM, Rich SS *et al.* Inflammatory and immune responses are impaired in mice deficient in intercellular adhesion molecule 1. Proc Natl Acad Sci USA 1993; **90**:8529–33.
23 Mayadas TN, Johnson RC, Rayburn H *et al.* Leukocyte rolling and extravasation are severely compromised in P-selectin-deficient mice. Cell 1993; **74**:541–54.
24 Cohen PL, Eisenberg RA. Lpr and gld: single gene models of systemic autoimmunity and lymphoproliferative disease. Annu Rev Immunol 1991; **9**:243–69.
25 Engelhardt B, Vestweber D, Hallmann R *et al.* E- and P-selectin are not involved in the recruitment of inflammatory cells across the blood–brain barrier in experimental autoimmune encephalomyelitis. Blood 1997; **90**:4459–72.
26 Engelhardt B, Laschinger M, Schulz M *et al.* The development of experimental autoimmune encephalomyelitis in the mouse requires alpha4-integrin but not alpha4beta7-integrin. J Clin Invest 1998; **102**:2096–105.
27 Kitagawa K, Matsumoto M, Mabuchi T *et al.* Deficiency of intercellular adhesion molecule 1 attenuates microcirculatory disturbance and infarction size in focal cerebral ischemia. J Cereb Blood Flow Metab 1998; **18**:1336–45.
28 Alexander EL, Murphy ED, Roths JB *et al.* Congenic autoimmune models of CNS disease in connective tissue disorders. Ann Neurobiol 1983; **14**:242–8.
29 Farrell M, Sakic B, Szechtman H *et al.* Effect of cyclophosphamide on leukocytic infiltration in the brain of MRL/lpr mice. Lupus 1997; **6**:268–74.
30 Wada T, Schwarting A, Chesnutt MS *et al.* Nephritogenic cytokines and disease in MRL-Fas (lpr) kidneys are dependent on multiple T-cell subsets. Kidney Int 2001; **59**:565–78.
31 Via CS, Shearer GM. Functional heterogeneity of L3T4$^+$ T cells in MRL-lpr/lpr mice. L3T4$^+$ T cells suppress major histocompatibility complex-self-restricted L3T4$^+$ T helper cell function in association with autoimmunity. J Exp Med 1988; **168**:2165–81.
32 Springer TA. Traffic signals of lymphocyte recirculation and leukocyte emigration: the multistep paradigm. Cell 1994; **76**:301–14.
33 Springer TA. Traffic signals on endothelium for lymphocyte recirculation and leukocyte emigration. Annu Rev Physiol 1995; **57**:827–72.
34 Vajkoczy P, Laschinger M, Engelhardt B. Alpha4-integrin-VCAM-1 binding mediates G protein-independent capture of encephalitogenic T cell blasts to CNS white matter microvessels. J Clin Invest 2001; **108**:557–65.
35 Kuhlman P, Moy VT, Lollo BA *et al.* The accessory function of murine intercellular adhesion molecule-1 in T lymphocyte activation. Contributions of adhesion and co-activation. J Immunol 1991; **146**:1773–82.
36 Van Seventer GA, Shimizu Y, Horgan KJ *et al.* The LFA-1 ligand ICAM-1 provides an important costimulatory signal for T cell receptor-mediated activation of resting T cells. J Immunol 1990; **144**:4579–86.
37 Kanwar S, Smith CW, Kubes P. An absolute requirement for P-selectin in ischemia/reperfusion-induced leukocyte recruitment in cremaster muscle. Microcirculation 1998; **5**:281–7.
38 Bullard DC, Mobley JM, Justen JM *et al.* Acceleration and increased severity of collagen-induced arthritis in P-selectin mutant mice. J Immunol 1999; **163**:2844–9.
39 Rosenkranz AR, Mendrick DL, Cotran RS *et al.* P-selectin deficiency exacerbates experimental glomerulonephritis: a protective role for endothelial P-selectin in inflammation. J Clin Invest 1999; **103**:649–59.
40 Frenette PS, Mayadas TN, Rayburn H *et al.* Susceptibility to infection and altered hematopoiesis in mice deficient in both P- and E-selectins. Cell 1996; **84**:563–74.

41 Staite ND, Justen JM, Sly LM *et al.* Inhibition of delayed-type contact hypersensitivity in mice deficient in both E-selectin and P-selectin. Blood 1996; **88**:2973–9.
42 Wolburg K, Gerhardt H, Schulz M *et al.* Ultrastructural localization of adhesion molecules in the healthy and inflamed choroid plexus of the mouse. Cell Tissue Res 1999; **296**:259–69.
43 McMurray RW. Adhesion molecules in autoimmune disease. Semin Arthritis Rheum 1996; **25**:215–33.
44 Poon BY, Ward CA, Giles WR *et al.* Emigrated neutrophils regulate ventricular contractility via alpha4 integrin. Circ Res 1999; **84**:1245–51.
45 Wong J, Johnston B, Lee SS *et al.* A minimal role for selectins in the recruitment of leukocytes into the inflamed liver microvasculature. J Clin Invest 1997; **99**:2782–90.
46 Downey GP, Worthen GS, Henson PM *et al.* Neutrophil sequestration and migration in localized pulmonary inflammation. Capillary localization and migration across the interalveolar septum. Am Rev Respir Dis 1993; **147**:168–76.
47 De Vriese AS, Endlich K, Elger M *et al.* The role of selectins in glomerular leukocyte recruitment in rat anti-glomerular basement membrane glomerulonephritis. J Am Soc Nephrol 1999; **10**:2510–7.